11th World Congress on Computational Mechanics (WCCM XI)
5th European Conference on Computational Mechanics (ECCM V)
6th European Conference on Computational Fluid Dynamics (ECFD VI)
July 20–25, 2014, Barcelona, Spain

STRONG DISCONTINUITY METHOD APPLIED TO SOIL/STRUCTURE INTERACTION IN EARTHQUAKE ENGINEERING

S. Cherubini[1], B. Richard[2], A. Frau[3]

[1] CEA, DEN, DANS, DM2S, SEMT, Laboratoire d'Etudes de Mecanique Sismique, F-91191 Gif sur Yvette, Stefano.Cherubini@cea.fr
[2] CEA, DEN, DANS, DM2S, SEMT, Laboratoire d'Etudes de Mecanique Sismique, F-91191 Gif sur Yvette, Benjamin.Richard@cea.fr
[3] CEA, DEN, DANS, DM2S, SEMT, Laboratoire d'Etudes de Mecanique Sismique, F-91191 Gif sur Yvette, Alberto.Frau@cea.fr

Key words: *Strong Discontinuity Method, Soil/structure interaction, Earthquake Engineering, Cast3M*

1 Introduction

When considering external forces acting on the foundation of a building, neither the structural displacements nor the ground displacements, are independent of each other. This inter-dependency phenomenon is known as soil-structure interaction (SSI). In particular, uplift between the soil and the foundation may occur during a seismic loading, leading to stability issues of the equipments located in the building. Therefore, it is of primary importance to take into account uplift in the early stage of the design process of a new building. Among the different approaches used to solve the SSI problems, we can notice the Winkler's methodologies, which lie in considering a spatial distribution of non-linear springs under the foundation [1, 2]. Despite the fact that this methodology is efficient, it does not provide any explicit quantitative description of the displacement jump due to uplift. An alternative method lies in considerering macroelements enhanced with complex constitutive laws to deal with dissipative mechanisms [3, 4]. The main problems of this method consist in identifying a large number of parameters, in addition to the fact that the quantification of the discontinuity jump is allowed. Lastly, we can mention the contact methods [5, 6], which allow to solve the problems mentioned above. In these methods the boundary conditions may change and the Dirichlet or Neumann boundary conditions must be replaced by limitations (or stresses) without specifying the exact values of displacement (neither the boundary stresses). An example is the unilateral contact condition [7], whose physical justification can be provided in the case of a deformable solid body with a rigid obstacle that does not allow it to deform freely under loading. We can also

imagine a bilateral contact, with two or more bodies that can be in contact, or even the self-contact between two parts of the same solid body that come in contact due to the large displacement. An other class of methods to describe contact lies in introducing a displacement discontinuity that is not aligned with element boundaries [8]. This methods requires to correct the velocity field, which generally leads to convergence issues. The main objective of this study is to explore the possibility to use the SDM (Strong Discontinuity Methods) to deal with SSI problems through an implementation based on a joint finite element.

This paper is outlined as follows. In a first part, a brief overview of existing unilateral contact methods, focusing on those that are used for the numerical case-study, is prescribed. In the second part, we show in details our model based on the joint element, by presenting all the constitutive equations, implemented in Cast3M-CEA environment [9]. In the last part, we present a series of comparative results regarding our numerical case-study.

2 Overview of existing unilateral contact methods

Regarding the unilateral contact methods, there are different strategies to describe a limitation in the space of configuration: (i) the Lagrange multipliers method, (ii) the penalty method and (iii) the augmented Lagrangian method. The first is very suitable for the resolution of the class of optimization problems with Neumann or Dirichlet boundary conditions. The changing boundary conditions can considerably complicate the implementation of Lagrange multipliers method and make its convergence difficult. The penalty method is also highly used to solve contact problems, introducing some extra stiffness terms in the global stiffness matrix to force the numerical fulfilment of the contact conditions [10, 11, 12, 13]. Nevertheless, it suffers from a lack of physical meaning since the additional stiffness terms are not justified. In addition, the arbitrary increase of stiffness terms leads to an uncorrect estimation of high frequency content. For these reasons, this method is not considered in the following. Only the augmented Lagrangian method remains robust and, at the same time, able to converge to the exact solution without too much difficulty. In the following, we show the main equations of the augmented Lagrangian method.

2.1 The augmented Lagrangian method

The augmented Lagrangian method is used for solving constrained optimization problems. This method has certain similarities to penalty methods, but it adds on additional term to the unconstrained objective, that is a Lagrange multiplier. In practice, it increases the number of unknowns by adding to the DOFs the boundary unknown forces [14]. In static, we obtain a system of this type:

$$\begin{bmatrix} \mathbf{K} & \mathbf{C^T} \\ \mathbf{C} & \mathbf{0} \end{bmatrix} \begin{bmatrix} \mathbf{u} \\ \lambda \end{bmatrix} + \alpha \begin{bmatrix} \mathbf{C^T C} & \mathbf{0} \\ \mathbf{0} & \mathbf{0} \end{bmatrix} \begin{bmatrix} \mathbf{u} \\ \lambda \end{bmatrix} = \begin{bmatrix} \mathbf{F} \\ \mathbf{d} \end{bmatrix} + \alpha \begin{bmatrix} \mathbf{C^T d} \\ \mathbf{0} \end{bmatrix} \tag{1}$$

where $\mathbf{K}$ is the stiffness matrix, $\mathbf{C}$ is the kinematic constraint matrix, $\mathbf{u}$ is the displacement vector, $\mathbf{d}$ is the prescribed displacement vector, $\mathbf{F}$ is the force vector, λ is the Lagrange multiplier and $\alpha \in \mathbb{K}^+$. If $\alpha = 0$, we can obtain the well-known Lagrange multipliers method, which can be solved in two simple steps, if $\mathbf{K}$ is a positive-definite matrix:

$$\mathbf{u} = \mathbf{K}^{-1}(\mathbf{F} - \mathbf{C^T}\lambda), \quad \lambda = -(\mathbf{C}\mathbf{C}^T)^{-1}(\mathbf{d} - \mathbf{C}\mathbf{K}^{-1}\mathbf{F}) \tag{2}$$

2.2 The dynamic contact

The formulation of the dynamic problem can be considered as belonging to the static problems.

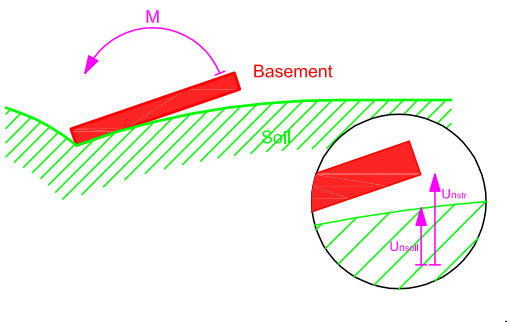

Figure 1: Uplift scheme (kinematic relation).

For instance, in a case of uplift at the soil-structure interface, a kinematic relation is prescribed:

$$u_n^{soil}(\mathbf{x}) - u_n^{str}(\mathbf{x}) \leq 0 \tag{3}$$

In a static case, an iterative resolution is considered to prescribe the kinematic relation where it is imposed. In a dynamic case, the kinematic condition must be fullfilled, but we must also ensure a velocity and acceleration field continuity. Mathematically, the latter is always verified, but not in a numerical computation. To verify this continuity, a velocity field correction is prescribed, through a lagrangian that ensures the equality of balance equation before and after contact [15]:

$$\begin{bmatrix} \mathbf{M} & \mathbf{C^T} \\ \mathbf{C} & \mathbf{0} \end{bmatrix} \begin{bmatrix} \dot{\mathbf{u}}' \\ \lambda \end{bmatrix} = \begin{bmatrix} \mathbf{M}\dot{\mathbf{u}}_{Lagrange} \\ \mathbf{0} \end{bmatrix} \tag{4}$$

where $\dot{\mathbf{u}}_{Lagrange}$ is the velocity field provided by the scheme. To take in account a certain propagation of the perturbation due to the contact, if the time step is not sufficiently small, we can write:

$$\begin{bmatrix} \mathbf{K} + \frac{4\mathbf{M}}{\Delta t^2} & \mathbf{C^T} \\ \mathbf{C} & \mathbf{0} \end{bmatrix} \begin{bmatrix} \dot{\mathbf{u}}'' \\ \lambda \end{bmatrix} = \begin{bmatrix} \mathbf{0} \\ 2\mathbf{C}(\dot{\mathbf{u}}' - \dot{\mathbf{u}}_{Lagrange}) \end{bmatrix} \tag{5}$$

and the corrected velocity field is expressed as follow:

$$\dot{\mathbf{u}}_c = \dot{\mathbf{u}}_{Lagrange} + \dot{\mathbf{u}}'' \tag{6}$$

3 The Strong Discontinuity Method

3.1 Displacement field

Let us consider a bidimensional body $\mathbf{\Omega} \subseteq \mathbb{R}^2$ whose material points are denoted as $\mathbf{x}$. Let us considerer the displacement field $\mathbf{u}$ defined, over $\mathbf{\Omega}$, by:

$$\mathbf{u}(\mathbf{x}) = \bar{\mathbf{u}}(\mathbf{x}) + \mathcal{H}(\mathbf{x})[\mathbf{u}](\mathbf{x}) \quad \mathbf{x} \in \Omega \tag{7}$$

where $\mathcal{H}(x)$ is defined as unit ramp function. In a kinematic state of strong discontinuity, when the discontinuity band collapses to the discontinuity line, $\mathcal{H}(x)$ becomes a step function $\mathcal{H}_s(x)$. The corresponding compatible strain field being:

$$\boldsymbol{\epsilon}(x) = \nabla^S \mathbf{u} = \underbrace{\nabla^S \bar{\mathbf{u}} + \mathcal{H}_S \nabla^S [\mathbf{u}]}_{\bar{\boldsymbol{\epsilon}}(<\infty)} + \underbrace{\delta_S ([\mathbf{u}] \otimes \mathbf{n})^S}_{[\boldsymbol{\epsilon}](>\infty)} \tag{8}$$

where δ_S is a Dirac's delta-function placed in discontinuity line S [7].

3.2 2D joint element formulation

The joint element, in fact dimensionless, does not have a local axis system. It is defined by the user and is arbitrary, consistent with the basis in which are expressed the Hooke's matrix and mass matrix coefficients. Because this is a problem of bond, the constitutive law links forces and displacements, differently from a classical approach. In 2D, the joint elements is made by two confounded lines.

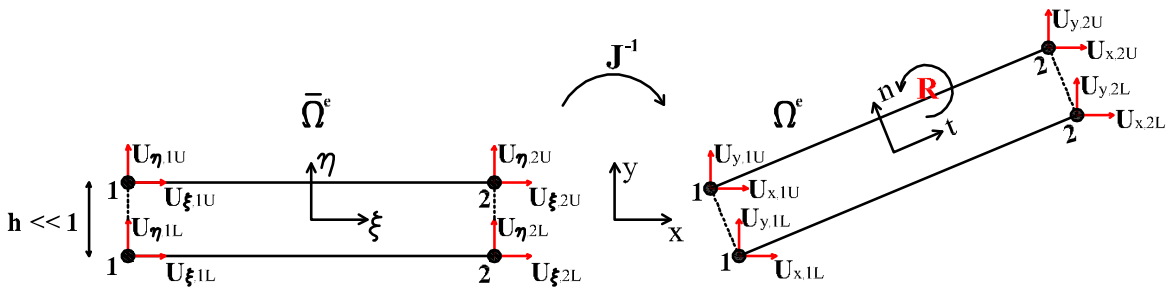

Figure 2: Reference scheme

The upper surface (indexed U) and the lower surface (indexed L) are defined from the element geometry:

$$\mathbf{x}_U = \sum_{i=1}^{n} N_i(\xi,\eta)\mathbf{x}_{i,U} \qquad \mathbf{x}_L = \sum_{i=1}^{n} N_i(\xi,\eta)\mathbf{x}_{i,L} \tag{9}$$

where N_i are the shape functions, $\mathbf{x}_i$ are the nodal coordinates of the element, n is the node number of each surface. Similarly, we can define the displacement fields of each element surfaces:

$$\mathbf{U}_U = \sum_{i=1}^{n} N_i(\xi,\eta)\mathbf{U}_{i,U} \qquad \mathbf{U}_L = \sum_{i=1}^{n} N_i(\xi,\eta)\mathbf{U}_{i,L} \tag{10}$$

The nodal element unknowns are the nodal displacements. Due to the non-existence of the element thickness, the element strains are defined as function of the relative displacements of the surfaces. To simplify the expression of internal element forces, we prefer working in the local system, tangent to the element surfaces.

$$\mathbf{u}_J = \mathbf{R}^{\mathbf{T}}\mathbf{U}_J, \quad J \in \{U, L\} \tag{11}$$

where $\mathbf{R} = [\mathbf{t}, \mathbf{n}]$; $\mathbf{t}$ and $\mathbf{n}$ are the unitary vectors that define the orthonormal tangent basis. In our case, the normal vector $\mathbf{n}$ is constant during the numerical computation. Now, we can define the element strains, or generalized strains:

$$\mathbf{u} = \begin{bmatrix} u_t \\ u_n \end{bmatrix} = \mathbf{u}_U - \mathbf{u}_L \tag{12}$$

Therefore, we can express the generalized strains in a matrix form function of $\tilde{\mathbf{u}}$, vector of nodal displacements, and matrix $\mathbf{B}$, computed from the shape functions N_i, as follows:

$$\mathbf{u} = \mathbf{B}\tilde{\mathbf{u}}, \quad \text{where} \quad \mathbf{B} = \begin{bmatrix} 1 & 0 & -1 & 0 \\ 0 & 1 & 0 & -1 \end{bmatrix}, \quad \tilde{\mathbf{u}} = \begin{bmatrix} \mathbf{u}_U \\ \mathbf{u}_L \end{bmatrix} \tag{13}$$

To allow the implementation within the framework of the modified Newton-Raphson resolution method, it is necessary to compute the internal nodal forces vector for each joint element as follows:

$$\mathbf{F} = \int_{\bar{\Omega}^e} \mathbf{B}^T \cdot \boldsymbol{\sigma} \cdot det(\boldsymbol{J}) \cdot d\xi d\eta \tag{14}$$

where $\boldsymbol{J}$ is the Jacobian matrix.

3.3 Constitutive law

To describe the material discontinuity behavior, the thermodynamic potential can be expressed according to [16]:

$$\rho\boldsymbol{\Psi}([\mathbf{u}], \xi) = \frac{1}{2}\eta[\mathbf{u}]\mathbf{K}[\mathbf{u}] + H(\xi) = \frac{1}{2}\eta[\mathbf{u}]\mathbf{K}[\mathbf{u}] - G_f(e^{-\frac{F_u}{G_f}\xi} - \xi\frac{F_u}{G_f}) + \alpha \tag{15}$$

where $[\mathbf{u}]$ is the discontinuity jump, H(ξ) is the consolidation function, $\mathbf{K}$ is the fourth-order Hooke's tensor, η is a closure function that is considered to gradually cancel the permanent displacements created in tension (which do not flow anymore) when unloading, F_u is the ultimate tensile force and G_f is the cracking energy. We have chosen $H(\xi)$ to ensure a kinematic exponential hardening in accordance with the experimental results on quasi-brittle materials, which would provide a softening in the force-displacement curve.

3.3.1 State equations

We can obtained the mechanical behavior by differentiating the state potential with respect the state variables. The state laws can be expressed as:

$$\mathbf{F} = \rho\frac{\partial\boldsymbol{\Psi}}{\partial[\mathbf{u}]} = \eta\mathbf{K}[\mathbf{u}], \quad [\mathbf{u}] = \begin{bmatrix} [u]_n \\ 0 \end{bmatrix} \tag{16}$$

$$q = \rho \frac{\partial \mathbf{\Psi}}{\partial \xi} = \frac{\partial H(\xi)}{\partial \xi} = F_u(e^{-\frac{F_u}{G_f}\xi} - 1) \tag{17}$$

where **F** is the thermodynamic force associated with the displacement jump and q is the thermodynamic force associated with the kinematic hardening.

3.3.2 Failure criterion

The failure criterion is defined such that:

$$\Phi(F_n, q) = F_n - (F_u + q), \tag{18}$$

where $F_n = \mathbf{F}_{tot} \cdot \mathbf{n}$ and $\mathbf{F}_{tot} = \mathbf{F}_{el} + \mathbf{F}$. If the threshold function is positive, then the discontinuity is introduced.

3.3.3 Flow rules

The internal variables related to the constitutive law to be considered on the discontinuity are managed by well-known normality rules since an associative flow is assumed. They can be expressed as follows:

$$[\dot{\mathbf{u}}] = \dot{\lambda} \frac{\partial \Phi}{\partial F_n} = \dot{\lambda}, \quad \dot{\xi} = \dot{\lambda} \frac{\partial \Phi}{\partial q} = -\dot{\lambda} \tag{19}$$

where $\dot{\lambda}$ is a multiplier that can be computed from the consistency condition $\dot{\Phi} = \Phi = 0$.

3.3.4 Unilateral effect

The unilateral effect can be considered through the function η, that ranges from 1 (cracks opened) to 0 (cracks closed) [17]. The following linear function is considered:

$$\eta = \begin{cases} 1 & \text{if } F_n > 0, \\ 1 - \frac{F_n}{F_c} & \text{if } F_c \leq F_n \leq 0, \\ 0 & \text{if } F_n < F_c, \end{cases} \tag{20}$$

where F_c is a material parameter that can be interpreted as the closure stress. In figure 3, we show the force-discontinuity curve for a tensile/compression test, where $[u]_{max}$ is defined as follows:

$$[u]_{max} := max_{\tau \in [0,t]}\{[u](\tau)\} \tag{21}$$

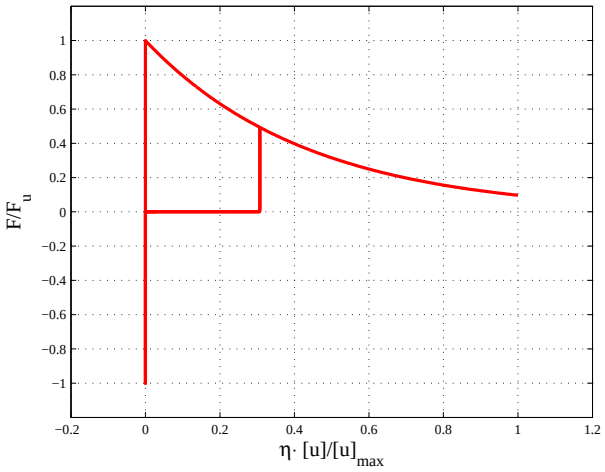

Figure 3: Cohesive force-discontinuity curve during.

4 Numerical case-study

Among the non-linear phenomena encountered in the SSI problems, some are related to the geometric non-linearity. The uplift at the soil-structure interface falls into this typology. Let us consider a simple oscillator. It is calibrated to obtain a natural frequency of 10 Hz under fixed condition. The mechanical characteristics are the followings: $E_{str} = 20000MPa$, $I_{str} = 0.20m^4$, $\nu_{str} = 0.3$. The mass M is computed to reach a first eigenfrequency equal to 10 Hz..

4.1 Dynamic inputs

A vertical force is prescribed at the top of the oscillator. In addition, a horizontal impulse is prescribed at the same point.

4.2 Dynamic outputs

In figures 5,6 and 7, we show a series of comparative results between the augmented Lagrangian method with two different type of velocity field correction (red for the Lagrangian augmented method with an accurate velocity field correction 'Unil. Cont.' and

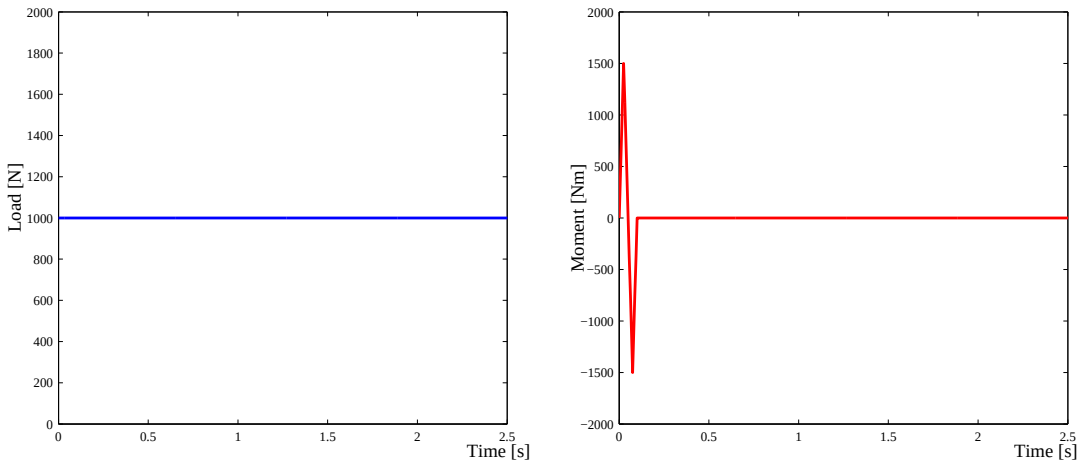

Figure 4: **a)** Load/Time curve, **b)** Moment/Time curve.

green for the Lagrangian augmented method with a non-accurate velocity field correction 'Unil. Cont. Err.') and the SDM (blue 'SDM').

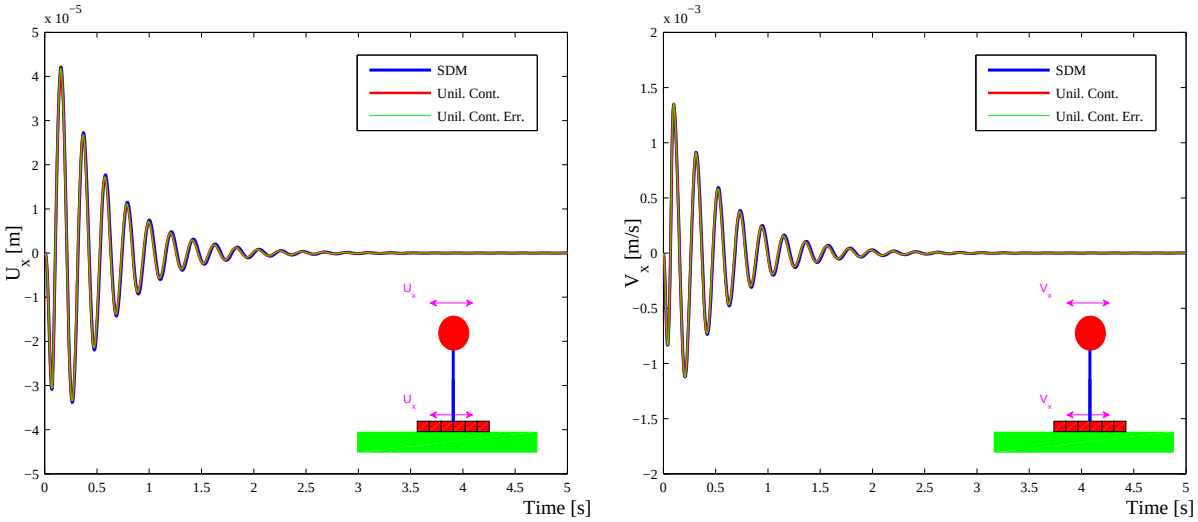

Figure 5: **a)** Displacement/Time curve, **b)** Velocity/Time curve.

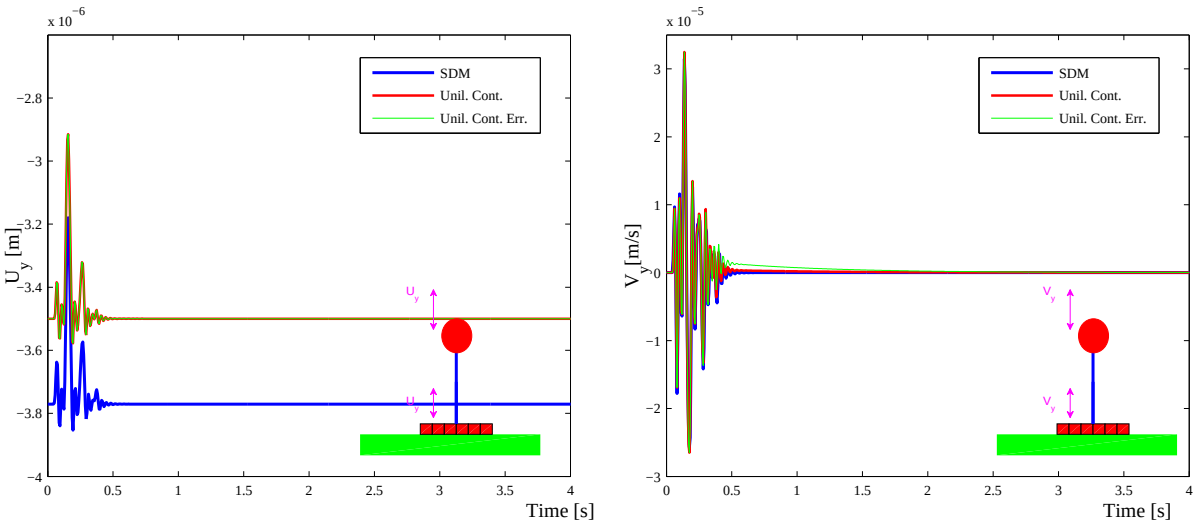

Figure 6: **a)** Displacement/Time curve, **b)** Velocity/Time curve.

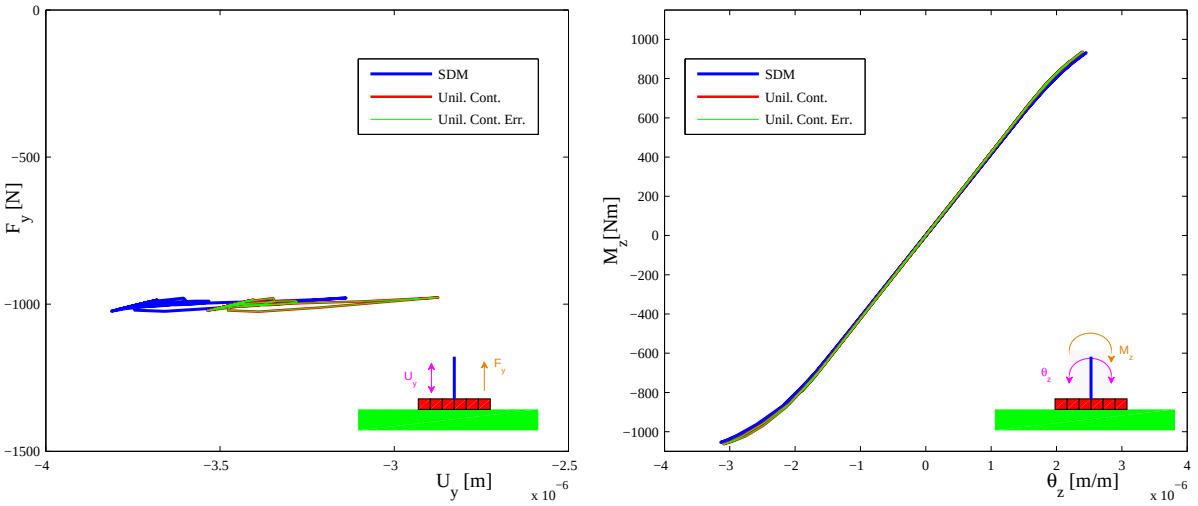

Figure 7: **a)** Force/Displacement curve, **b)** Moment/Curvature curve.

By observing the results, it is clear that the responses obtained with the augmented Lagrangian method are strongly influenced by the velocity field correction. To remark this, in the figure 8 we have only compared the two results obtained with the Lagrangian method for a null damping, condition that emphasizes the great difference due to the velocity field correction.

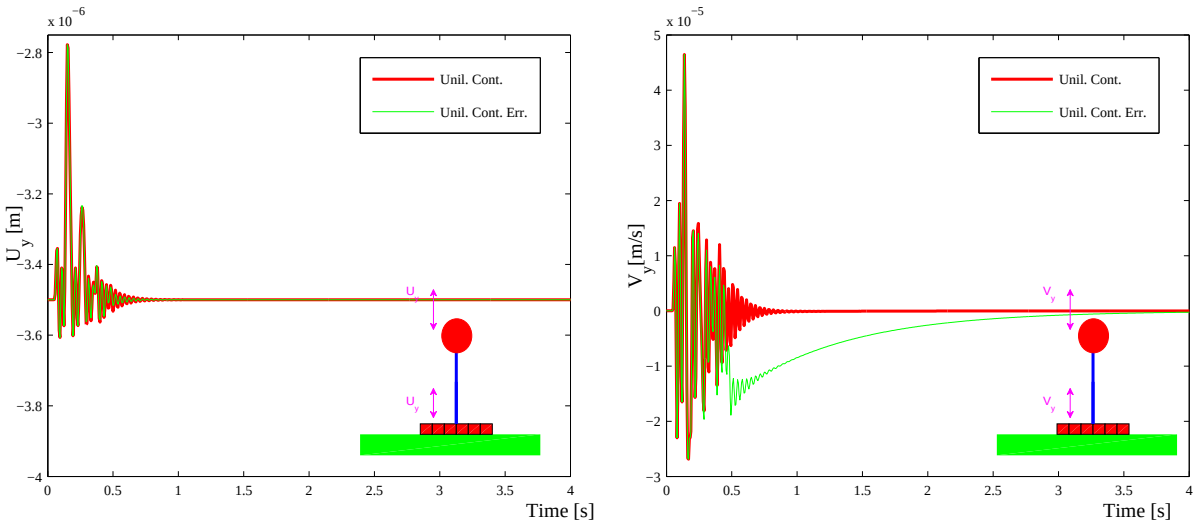

Figure 8: **a)** Displacement/Time curve, **b)** Velocity/Time curve.

5 Conclusion and outlooks

In this paper, the possibility to use the SDM to deal with SSI problems has been investigated. From the elementary structural case study presented, the following conclusions could be drawn: (i) the SDM seems to provide a robust numerical solution with an explicit quantification of the displacement jump considering uplift and (ii) the velocity field does not require specific correction anymore. These first results make the Authors confident for further works. As the main perspective of this study, the implementation of a 3D version of the proposed constitutive law is under study, leading to possibility to deal with real structures that may have an asymmetric shape.

Acknowledgments

The research reported in this paper has been supported in part by the SEISM Paris Saclay Research Institute.

REFERENCES

[1] Apostolu M., Gazetas G., Garini E., Seismic response of slender rigid structures with foundation uplifting, *Soil Dynamics and Earthquake Engineering*, Vol. **27**, 642–654, 2007

[2] Psycharis I. N., Investigation of dynamic response of rigid footings on tensionless Winkler foundation, *Soil Dynamics and Earthquake Engineering*, Vol. **28**, 577–591, 2008

[3] Cremer C, Pecker A., Davenne L., Modelling of nonlinear dynamic behavior of a

shallow strip foundation with macro-element. *Journal of Earthquake Engineering*, Vol. **6**(2), 175–211, 2002

[4] Grange S., Kotronis P., Mazar J., A macro-element for a circular foundation to simulate 3D soil-structure interaction, *International Journal for Numerical and Analytical Methods in Geomechanics*, Vol. **32**, 1205–1227, 2008

[5] Oliver, J. On the discrete constitutive models induced by strong discontinuity kinematics and continuum constitutive equations. *International Journal of Solids and Structures*, Vol. **37**(48), 7207–7229, 2000.

[6] Oliver, J., Huespe, A. E. Theoretical and computational issues in modelling material failure in strong discontinuity scenarios. *Computer Methods in Applied Mechanics and Engineering*, Vol. **193**(27), 2987–3014, 2004.

[7] Polizzotto C., Zito M., BIEM - based variational principles for elastoplasticity with unilateral contact boundary conditions, *Engineering Analysis with Boundary Elements*, Vol. **21**, 329–338, 1998

[8] Oliver J., Cervera M., Manzoli O., Strong discontinuities and continuum plasticity models: the strong discontinuity approach, *International Journal of Plasticity*, Vol. **15**, 319–351, 1999

[9] www-cast3m.cea.fr

[10] Gonzalez Jose A., Park K.C., Felippa Carlos A., Abascal R., A formulation based on localized Lagrange multipliers for BEM-FEM coupling in contact problems, *Comput. Methods Appl. Mech. Engrg.*, Vol. **197**, 623–640, 2008

[11] Amdouni S., Moakher M., Renard Y., A stabilized Lagrange multiplier method for the enriched finite-element approximation of Tresca contact problems of cracked elastic bodies, *Comput. Methods Appl. Mech. Engrg.*, Vol. **270**, 178–200, 2014

[12] Oysu C., Fenner Roger T., Coupled FEM-BEM for elastoplastic contact problems using Lagrange multipliers, *Applied Mathematical Modelling*, Vol. **30**, 231–247, 2006

[13] Clark B.W., Anderson D.C., The penalty boundary method, *Finite Elements in Analysis and Design*, Vol. **39**, 387–401, 2003

[14] Carpintieri A., Ferro G., Ventura G., An augmented Lagrangian element-free (ALEF) approach for crack discontinuities, *Comput. Methods Appl. Mech. Engrg.*, Vol. **191**, 941–957, 2001

[15] Hughes T.J.R., Taylor R.L., Sackman J.L., Curnier A., Kanaknukulchai W., A finite element method for a class of contact-impact problems, *Comput. Methods Appl. Mech. Engrg.*, Vol. **8**, 249–276, 1976

[16] Oliver J., Huespe A.E., Pulido M.D.G., Chaves E., From continuum mechanics to fracture mechanics: the strong discontinuity approach, *Engineering Fracture Mechanics*, Vol. **69**, 113–136, 2002

[17] Richard B., Ragueneau F., Continuum damage mechanics based model for quasi brittle materials subjected to cyclic loadings: Formulation, numerical implementation and applications, *Engineering Fracture Mechanics*, Vol. **98**, 383–406, 2013